Available online at www.sciencedirect.com
SCIENCE DIRECT
Chemometrics and Intelligent Laboratory Systems 82 (2006) 276 – 282
Chemometrics and intelligent laboratory systems
www.elsevier.com/locate/chemolab

Automatic tracking of biological cells and compartments using particle filters and active contours

Hailin Shen [a], Glyn Nelson [b], Stephnie Kennedy [b], David Nelson [b], James Johnson [b], David Spiller [b], Michael R.H. White [b], Douglas B. Kell [a,*]

[a] School of Chemistry, The University of Manchester, Faraday Building, Sackville St., PO Box 88, Manchester, M60 1QD, UK
[b] Centre for Cell Imaging, School of Biological Sciences, Bioscience Research Building, Crown St., Liverpool, L69 7ZB, UK

Received 8 February 2004; received in revised form 6 July 2005; accepted 6 July 2005
Available online 9 December 2005

Abstract

In order to gain a detailed understanding of cell signalling and regulation processes, live cell imaging is often used. Such signalling can involve the nuclear-cytoplasmic translocation of signalling molecules, and to follow this, it is necessary to mark the cell and nuclear boundaries in an image sequence in individual cells. For complex processes, with both rapid cell motion and nuclear translocation, it is extremely time-consuming to mark such cell boundaries manually. The particle filter (PF) is a Monte Carlo method based on sequential importance sampling. It is robust to clutter and the occlusion of targets in object tracking. The active contour (AC) method is based on a deformable model and is capable of capturing minor cell shape variations, although a good initialisation is often required. Prior information from a particle filter provides a reasonable initialisation for the active contour method and prevents it from being trapped in local minima. Combining these two methods (PF-AC) thus makes it possible to track complex cellular processes automatically. The combined method is used to study the important NF-κB signalling pathway. Comparable results to those obtained manually by a biologist are obtained using the hyphenated approach, but in a small fraction of the time.

Keywords: Cell signalling pathway; Tracking; Active contour; Particle filter; NF-κB

1. Introduction

The function of most genes in humans (and even in lower organisms) remains unknown, despite the successful systematic genome sequencing programmes [1]. This has ushered in the era of high-throughput biology as a means to establish gene functions. Recent developments in biology now make it possible to screen thousands of gene products 'simultaneously' for their role in biological processes such as cell division, signalling pathways and gene expression; this is done with the help of fusion proteins, e.g. those based on GFP (green fluorescent protein) [2]. Hundreds or thousands of images may be generated in such experiments and fast image analysis is then essential for high-throughput functional gene analysis.

NF-κB proteins are small groups of closely related transcription factors, which in mammals consist of five members: Rel (also known as c-Rel), RelA (also known as p65 and NF-κB3), RelB, NF-κB1 (p50) and NF-κB2 (p52). These related members are critical regulators of cell division, apoptosis and inflammation. The NF-κB signalling pathway is an important pathway, in which protein phosphorylation leads to the activation of further downstream events [3–6]. Recent studies have suggested that NF-κB signalling involves oscillations of NF-κB between the cytoplasm and nucleus of cells and that these oscillations are required for the maintenance of gene expression [6,7]. Fig. 1 shows a typical HeLa cell displaying changes in both the location and concentration of DsRed-tagged NF-κB. Its neighbouring cells will typically be at different phases in the oscillatory signalling dynamics and thus individual cells must therefore be studied (as averaging between cells will obscure the oscillations). To track such cell activities, one has to mark single cell boundaries on each frame

* Corresponding author. Tel.: +44 161 306 4492; fax: +44 161 306 4556.
E-mail address: dbk@manchester.ac.uk (D.B. Kell).
URL: http://dbk.ch.umist.ac.uk (D.B. Kell).

0169-7439/$ - see front matter © 2005 Elsevier B.V. All rights reserved.
doi:10.1016/j.chemolab.2005.07.007

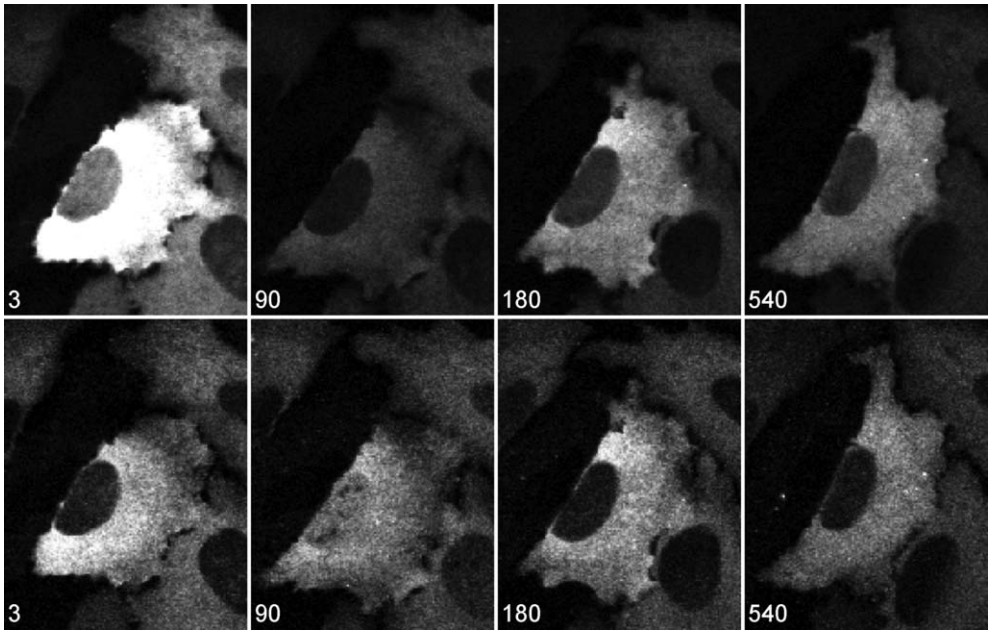

Fig. 1. One typical HeLa cell in NF-κB signalling control at 0, 90, 180 and 540 min. The upper row images show the cell expressing a fusion protein of EGFP to IκBα and the lower row images show the DsRed fusion protein to RelA.

and this is then an object tracking problem from the point of view of the computer vision community. As can be seen from Fig. 1, the cells overlap and the shapes of boundaries vary irregularly over time, i.e. they are non-rigid. It is extremely tedious, time-consuming and potentially error-prone to mark the cell boundaries manually, and it is thus essential to apply tracking techniques to enable fast analysis. Note that we try to track cell boundaries without using any dye to help the tracking process, since the added dye may hinder the normal cell cycles.

Tracking objects in an image sequence is one of the basic tasks in computer vision [8]. Tracking algorithms often use two sources of information: a model of the dynamical behaviour of the object being tracked (dynamic model) and a model of its appearance within an image (appearance model). Both can be acquired from a representative training set. In addition to dynamic and appearance models, an observation model is often required to evaluate the fitness of a hypothetical object appearance given a set of image features. However, cell appearance and fluorescent intensity may vary wildly during cell signalling processes such as those of present interest. It is therefore desirable to track cell boundaries instead of the whole cellular region. The use of an edge (contour) based algorithm may serve for this purpose. The tracking process involves finding an object shape model, leading to robust estimates of the object position and shape. The classic formulation of this approach is contour tracking via a Kalman filter [9]. Tracking methods based on Kalman filters assume that dynamic and measurement models are linear with Gaussian noise. However, for cellular image sequences, there are many interfering factors, e.g. background clutter and occluding objects, and it is hard to produce clean edges corresponding only to cellular boundaries. This often causes the collapse of Kalman filter tracking strategies [10]. A very robust algorithm is therefore required to obtain reliable results.

The particle filter is a robust approach that has recently enjoyed considerable success [10,11]. The particle filter does not require the assumption of a Gaussian distribution and the dynamic and measurement models may also be nonlinear. It is based on creating an approximation to the full probability distribution of the object's configuration over all possible locations using random sampling. This enables them to retain multimodal probability distributions, making them robust to temporarily ambiguous image support and hence able to maintain tracking even in the presence of clutter and occlusions. They also have the advantage of being simple to implement [12]. However, cells are not rigid objects with simple shapes. A more accurate result is expected to accommodate some non-rigid variations.

The active contour (AC), first introduced by Kass et al. [13], considers curves defined within an image domain that can

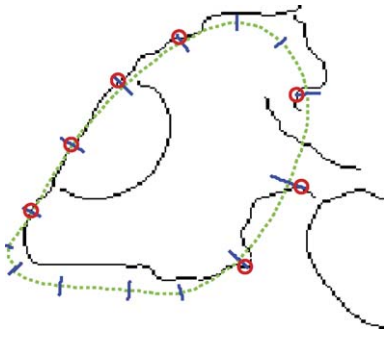

Fig. 2. Observation model using the Canny edge detector (---: hypothetical contour; —: normal lines; o: observed edge points).

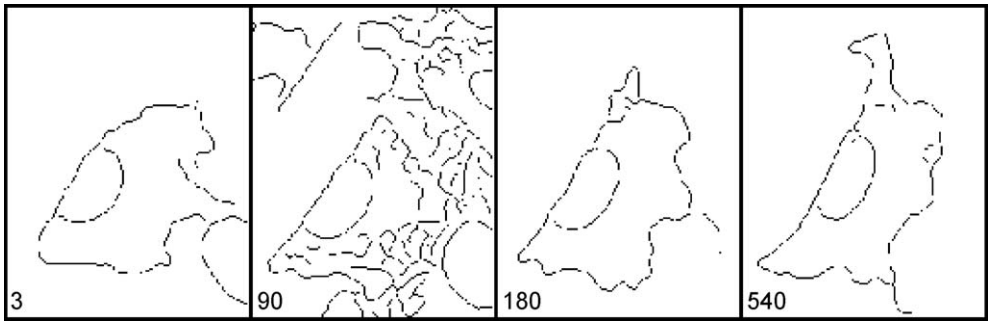

Fig. 3. Binary image edges as obtained by the Canny edge detector for the images in the upper row of Fig. 1.

move under the influence of internal forces within the curve itself and external forces derived from the image data. The active contour has found many applications, including edge detection [14] and motion tracking [15]. No shape model is imposed in the active contour method. It is therefore suitable for irregular non-rigid objects. However, the initial contour must, in general, be close to the true boundary or else it will likely converge to the wrong result. Thus, a prior result from the particle filter may be expected to provide a good initialisation. The active contour then acts as a post processing in this application.

Computer vision techniques, e.g. active contour, have enjoyed a number of applications in biomedical science, but they are mainly in the field of static image segmentation [16]. In motion analysis, cells are often simplified as a point or circular object or stained with cytoplasmic or nuclear dyes, which may hinder their normal cell cycles. In this application, no cytoplasmic or nuclear dyes were added to assist cell re-

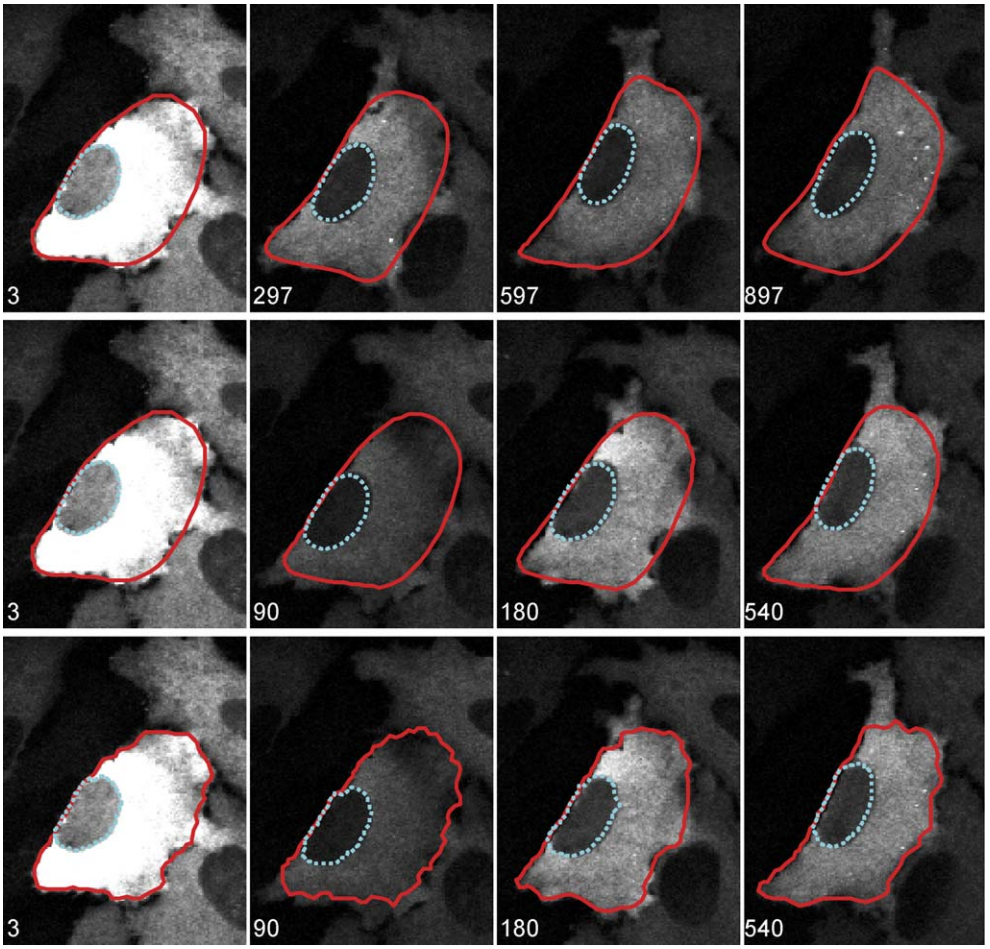

Fig. 4. Cell boundary tracking. Initial boundaries on key frames (upper row), obtained by the PF (middle) and the one obtained by PF-AC (lower row). —: cytoplasmic boundary; . . .: nuclear boundary.

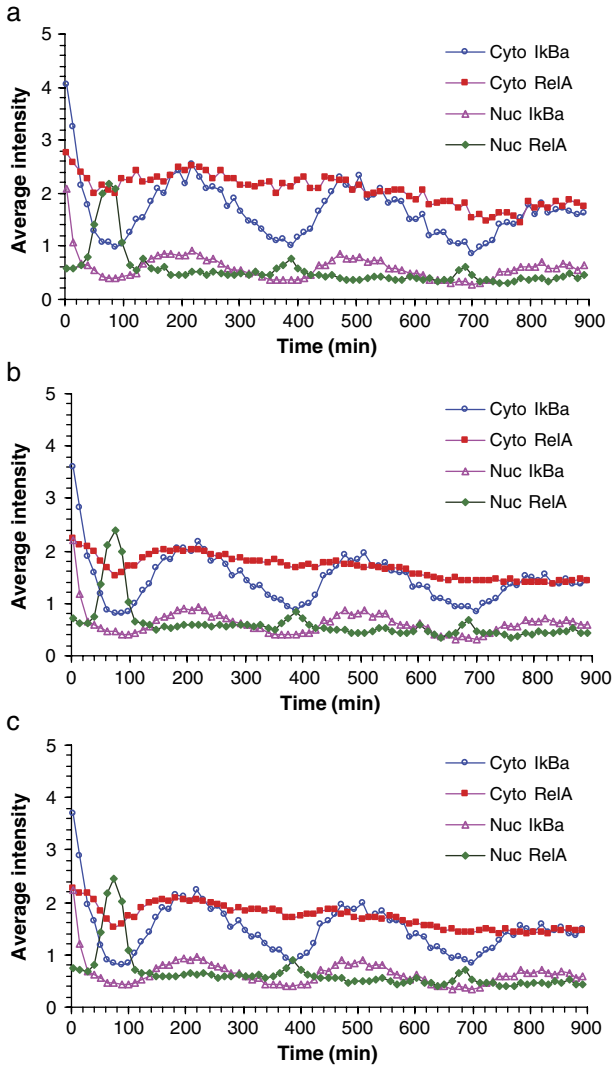

Fig. 5. Fluorescent profiles for the cytoplasmic and nuclear amounts of RelA and IκBα obtained by a biologist (a), by PF (b) and by PF-AC (c).

cognition. To the authors' knowledge, this is the first application of either particle filter or active contour methods in single cell signalling pathway tracking.

2. Theory

In contour-based particle filter tracking, one has to define a shape model, a dynamic model and an observation model. A cell boundary may consist of tens of points, since it is impractical to track all the points individually. Tracking is often limited to just a few parameters by building a shape model. The fitness of a boundary is evaluated using an observation model.

2.1. Shape model

In many tracking applications, object shape is modelled using 2D planar affine transform [12] with only one shape template. In most cases, the nuclear boundaries undergo limited changes, which may be also modelled using the conventional approach. The variation of cytoplasm boundaries is, however, non-rigid, a model using only one shape template is usually insufficient. We notice that the shape change is usually steady over the time course. The cellular boundary may be approximated by a linear combination of those on the key frames; thus, one uses a couple of representative boundaries as templates. Any allowed shape vector $\boldsymbol{Q}$ between key frames 1 and 2 can be written as

$$\boldsymbol{Q} = \boldsymbol{W}\boldsymbol{s} \tag{1}$$

$$\boldsymbol{W} = \begin{bmatrix} \boldsymbol{1} & \boldsymbol{0} & \boldsymbol{Q}_1^x & \boldsymbol{Q}_2^x \\ \boldsymbol{0} & \boldsymbol{1} & \boldsymbol{Q}_1^y & \boldsymbol{Q}_2^y \end{bmatrix}. \tag{2}$$

Here $\boldsymbol{s}$ is a vector for estimating $\boldsymbol{Q}$ within the shape space defined by $\boldsymbol{W}$. $\boldsymbol{1}$ and $\boldsymbol{0}$ in Eq. (2) are vectors with 1s and 0s, respectively. $\boldsymbol{Q}^x$ and $\boldsymbol{Q}^y$ are the x, y coordinates of shape template on the key frames. The first two columns of $\boldsymbol{W}$ govern horizontal and vertical translations, respectively. The third and fourth columns, made up from the templates, cover shape variations in the x and y directions. $\boldsymbol{Q}^x$ and $\boldsymbol{Q}^y$ are chosen to have their centroids at the origin so that the third and fourth columns are associated with shape changes only. The weight matrix $\boldsymbol{W}$ will be updated once a new key frame appears. In doing so, the weight matrix covers only changes between neighbouring key frames.

2.2. Dynamic model

We assume that the cell boundaries vary steadily over time. The shape changes between frames, $\Delta\boldsymbol{s}$, may be calculated beforehand. Note that here the position information is excluded since templates have their centroid at the origin. We have to set a large noise level to the position elements of ε_k at the time k, in order to cover the possible motion range. A small random amount of shape variation is added as well because the shape change is not necessarily evenly distributed between the key frames.

$$\boldsymbol{s}_k = \boldsymbol{s}_{k-1} + \Delta\boldsymbol{s} + \boldsymbol{e}_k \tag{3}$$

2.3. Observation model

The image feature used in this paper is the set of edges obtained from the Canny edge detector [17]. Given an image, the Canny edge detector produces a binary image with the detected object edges as the foreground. Observation is done along the normals at certain contour points. For the sake of convenience, these points are evenly spaced in this application.

Table 1
Pearson correlation coefficient of profiles obtained manually and those by PF and PF-AC

	Cyto IκBα	Cyto RelA	Nuc IκBα	Nuc RelA
PF	0.988	0.923	0.985	0.985
PF-AC	0.987	0.904	0.987	0.988

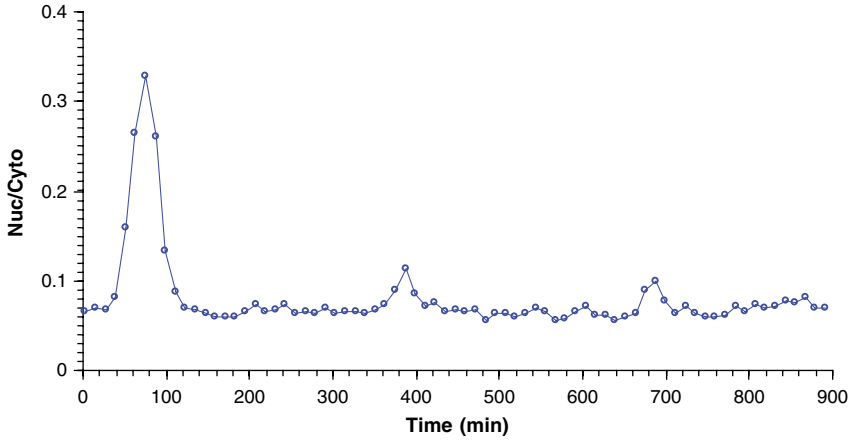

Fig. 6. Ratio of average DsRed (fused with RelA) fluorescent intensity between nucleus and cytoplasm over time.

Given edges detected along a normal of the contour, its probability of being a true contour point is determined as follows [12].

$$p \propto 1 + \frac{1}{\sqrt{2\pi}\sigma\lambda} \sum_{m=1}^{M} e^{-\frac{f(d_m,\mu)}{2\sigma^2}} \text{ where } f(d_m,\mu) = \min\left(d_m^2, \mu^2\right). \quad (4)$$

The parameter σ, similar to the standard deviation in a normal distribution, is set according to the accuracy of the shape model. The more accurate a shape model, the smaller σ is. λ is related to the prior probability of the contour point not being detected by edge detection. d_m is the distance between the contour and the edge along its mth normal. μ is the maximum distance between the contour and edge points under consideration. The probability of a hypothetical contour aligning with the true contour is estimated by multiplying the probabilities of edges along all the normal lines. Fig. 2

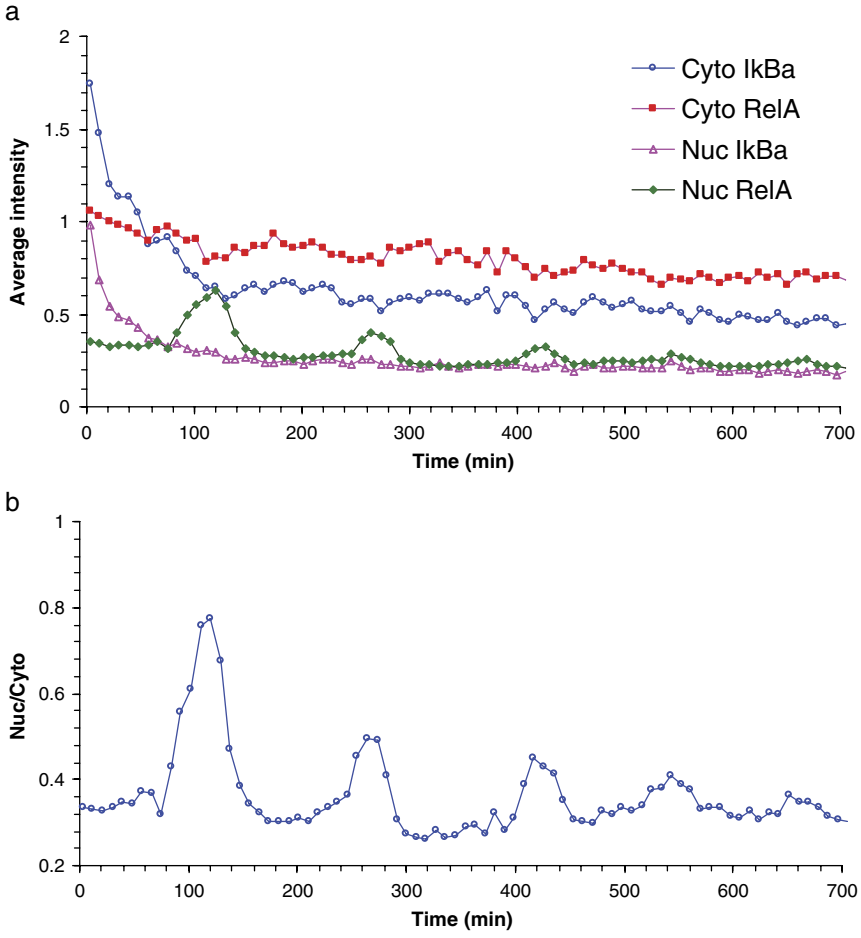

Fig. 7. Fluorescent profiles of another HeLa cell using PF-AC (a) and the ratio of average DsRed fluorescent intensities between nucleus and cytoplasm (b).

illustrates the observation model using the 3-min image in Fig. 1. If there is no edge detected, as we can see from Eq. (4), $f(d_m,\mu)=\mu^2$.

2.4. Particle filter tracking

Object tracking can be characterised as the problem of estimating the state of a system given a set of observations. The state refers to the positions and shape parameters of contours in this application. The observation is represented by the image edges of each frame. We define $\boldsymbol{s}$ the state vector consisting of a contour's position and orientation and $\boldsymbol{z}$ measurement vector with image edge locations. Notation $p(\boldsymbol{z}|\boldsymbol{s})$ is the probability of measuring $\boldsymbol{z}$ given state $\boldsymbol{s}$. The aim of tracking is to estimate recursively in time the posterior probability density $p(s_k|z_{1:k})$ when $k=1,2,\ldots$, and the associated expectation of some integral function $g_k(s_k)$, which is computed as

$$E(g_k(s_k)) = \int g_k(s_k)p(s_k|z_{1:k})\mathrm{d}s_k. \quad (5)$$

In most cases involving non-Gaussianity and nonlinearity, analytical solutions to Eq. (5) are impossible. In the particle filter, a proposed density $\pi(s_k|z_{1:k})$ is used where N random states are simulated. Eq. (5) is formulated as

$$E(g(s))\frac{1}{N}\sum_{n=1}^{N} g\left(s^{(n)}\right)\underbrace{\frac{p\left(s^{(n)}\right)}{\pi\left(s^{(n)}\right)}}_{\text{weight}} \quad (6)$$

The tracking procedure can be implemented as follows [10]:

1. Generate N state vectors based on the target cell boundary using the dynamic model.
2. Compute the weight (probability) of each contour using Eq. (4) and normalise the weight over the state population.
3. Estimate the state vector $\boldsymbol{s}$expectation using Eq. (6) where $g(\boldsymbol{s})=\boldsymbol{s}$. Use the recent state estimation to initialise the tracking of the next frame. Go to step 1 until the tracking finishes.

2.5. GVF active contour

The active contour [13] is a curve $\chi(r)=[x(r), y(r)]$ that moves within an image to minimize the energy function

$$E = \int_0^1 \left(\alpha|\chi'(r)|^2 + \beta|\chi''(r)|^2 + E_{\text{ext}}(\chi(r))\right)\mathrm{d}r \quad (7)$$

where α, β specify the elasticity and stiffness of the active contour. The external energy function E_{ext} is derived from the image so that it takes on its smaller values at the features of interest, such as boundaries. There are quite a few formulations of the active contour. In the algorithm developed by Xu and Prince [14], the external force is defined as the gradient vector flow (GVF) field. The main advantages of GVF active contours are: (1) a longer capture range to guide the contour towards the desired boundary and (2) an ability to progress into boundary concavities. The latter is very useful since cell boundaries may have sharp corners, a feature that has not been covered by the shape model in particle filter tracking.

3. Data and software

The experimental details of how the NF-κB time series images were acquired are given in [6]. The quantitative information of the location and amount of tagged IκBα and RelA (p65) are obtained using enhanced green fluorescent protein (EGFP) and DsRed, respectively. All the programmes are implemented in Tracker, a Matlab (The MathWorks, Inc.) package developed by the first author using Matlab™ 7.0 with its image processing toolbox.

4. Results and discussion

The active contour method is an approach to generate curves that move within images to find object boundaries. It is a non-rigid method suitable for refining complex object boundaries provided it is given a good initialisation. Fig. 3 shows the edges of those images in Fig. 1 as obtained using the Canny edge detector. In the ideal case, edges detected by this method will correspond to object boundaries. However, due to clutter and inhomogeneous distributions of image intensity within cellular compartments, it is very difficult to obtain clean edges associated with cell boundaries alone.

Fig. 4 shows the marked boundaries on the key frames at 3, 297, 597 and 897 min (upper row). The middle and lower row subplots are the tracking results of the typical frames in Fig. 1. For the key frame at 3 min, the result of the particle filter is the same as the initial boundaries. The boundaries at the frames at 90 and 180 min are a linear combination of key frames at 3 and 297 min. The former are very similar to those on the frame at 3 min. The latter bears more features of the boundaries at 297 min. After the active contour processing, the boundaries align themselves with the local edges. The algorithm is complementary to the simple shape model in the particle filter. The result of particle filter in Fig. 5 shows the EGFP and DsRed fluorescent profiles obtained by a biologist (one of the authors), by PF and by PF-AC, respectively. They are quite similar, and the correlation coefficients between the latter two methods and the profiles obtained manually are shown in Table 1. It is obvious that the results from PF and PF-AC are comparable to those marked up manually by the human scientist. However, for the fluorescent profiles of cytoplamic RelA, the PF and PF-AC result is somewhat smoother compared to that obtained by the biologist. Fig. 6 shows the sampled oscillations observed in the averaged nuclear/cytoplasmic ratio of RelA. The plots clearly indicate that cell signalling in this study is periodic with a decaying response. Fig. 7 shows the results from another cell. The cytoplasmic and nuclear profiles are different from those in Fig. 6, because these two cells are at different signalling *phases*, reinforcing the importance of measuring single cells.

In NF-κB (here RelA) signalling processes [6,18], NF-κB is held inactive in the cytoplasm of non-stimulated cell by various IκB isoforms. During cell stimulation, the IKK (inhibitor kappa B kinase) complex is activated, leading to

phosphorylation and ubiquitination of the IκB proteins. Free NF-κB translocates to the nucleus, activating genes including IκBα, which contains nuclear localization and export sequences. This enables IκBα nuclear-cytoplasmic shuttling. Newly synthesised IκBα binds to nuclear NF-κB, leading to the export of the complex to the cytoplasm. This complex becomes the target for IκBα phosphorylation. In this application, NF-κB responds to TNFα (tumour necrosis factor alpha) simulation, giving rise to oscillations in fluorescent profiles of RelA [19], and it is the oscillations rather than the instantaneous concentrations that, as with p53 [20], may represent the signal that is detected downstream [21].

5. Conclusion

A hyphenated approach (PF-AC) has been applied to track cell signalling processes. It combines the robustness of the particle filter with the flexibility of active contour. The results show that this approach can be used successfully to track cell boundaries in complex cell signalling processes, even with overlapping cellular boundaries.

Acknowledgements

The authors thank the DTI (under the terms of the Beacon project), the BBSRC, EPSRC and RSC for financial support, and Steve O'Hagan of the Manchester group for help with reading Carl Zeiss LSM image data files.

References

[1] P. Hieter, M. Boguski, Science 278 (1997) 601–602.
[2] R.Y. Tsien, Annu. Rev. Biochem. 67 (1998) 509–544.
[3] A. Hoffmann, A. Levchenko, M.L. Scott, D. Baltimore, Science 298 (2002) 1241–1245.
[4] K.H. Cho, S.Y. Shin, H.W. Lee, O. Wolkenhauer, Genome Res. 13 (2003) 2413–2422.
[5] A. Ihekwaba, D.S. Broomhead, R. Grimley, N. Benson, D.B. Kell, Syst. Biol. 1 (2004) 93–103.
[6] D.E. Nelson, A.E.C. Ihekwaba, M. Elliott, C.A. Gibney, B.E. Foreman, G. Nelson, V. See, C.A. Horton, D.G. Spiller, S.W. Edwards, H.P. McDowell, J.F. Unitt, E. Sullivan, R. Grimley, N. Benson, D.S. Broomhead, D.B. Kell, M.R.H. White, Science 306 (2004) 704–708.
[7] D.E. Nelson, V. See, G. Nelson, M.R.H. White, Biochem. Soc. Trans. 32 (2004) 1090–1092.
[8] D.A. Forsyth, J. Ponce, Computer Vision: a Modern Approach, Prentice Hall, Upper Saddle River, NJ, 2003.
[9] A. Blake, M. Isard, D. Reynard, Artif. Intell. 78 (1995) 179–212.
[10] M. Isard, A. Blake, Int. J. Comput. Vis. 29 (1998) 5–28.
[11] N. Gordon, A. Doucet, N. De Freitas, Sequential Monte Carlo Methods in Practice, Statistics for Engineering and Information Science, Springer, New York, 2001.
[12] A. Blake, M. Isard, Active Contours: the Application of Techniques from Graphics, Vision, Control Theory and Statistics to Visual Tracking of Shapes in Motion, Springer, London, 1998.
[13] M. Kass, A. Witkin, D. Terzopoulos, Int. J. Comput. Vis. 1 (1987) 321–331.
[14] C.Y. Xu, J.L. Prince, IEEE Trans. Image Process. 7 (1998) 359–369.
[15] N. Ray, S.T. Acton, K. Ley, IEEE Trans. Med. Imag. 21 (2002) 1222–1235.
[16] T.F. Cootes, C.J. Taylor, D.H. Cooper, J. Graham, Comput. Vis. Image Underst. 61 (1995) 38–59.
[17] J. Canny, IEEE Trans. Pattern Anal. Mach. Intell. 8 (1986) 679–698.
[18] G. Nelson, L. Paraoan, D.G. Spiller, G.J.C. Wilde, M.A. Browne, P.K. Djali, J.F. Unitt, E. Sullivan, E. Floettmann, M.R.H. White, J. Cell Sci. 115 (2002) 1137–1148.
[19] M.W. Young, S.A. Kay, Nat. Rev. Genet. 2 (2001) 702–715.
[20] G. Lahav, N. Rosenfeld, A. Sigal, N. Geva-Zatorsky, A.J. Levine, M.B. Elowitz, U. Alon, Nat. Genet. 36 (2004) 147–150.
[21] D.B. Kell, Biochem. Soc. Trans. 33 (2005) 520–524.